Synthesis, Structures, and Spectroscopic, Magnetic, and Electrochemical Properties of (μ-Alkoxo)bis(μ-carboxylato)diruthenium Complexes, M[Ru_2(dhpta)(μ-$O_2CR)_2$] (M = Na and K, dhptaH_5 = 1,3-Diamino-2-hydroxypropanetetraacetic Acid)

Tomoaki Tanase,*,† Yasuko Yamada,‡ Keiko Tanaka,‡ Tomoko Miyazu,‡ Masako Kato,‡ Keomil Lee,§ Yoshikazu Sugihara,§ Wasuke Mori,§ Akio Ichimura,|| Isamu Kinoshita,|| Yasuhiro Yamamoto,† Masaaki Haga,⊥ Yoichi Sasaki,& and Shigenobu Yano*,‡

Department of Chemistry, Faculty of Science, Nara Women's University Nara-shi, Nara 630, Japan, Department of Chemistry, Faculty of Science, Toho University, Miyama, Funabashi-shi, Chiba 274, Japan, Department of Chemistry, Faculty of Science, Osaka University, Toyonaka-shi, Osaka 560, Japan, Department of Chemistry, Faculty of Science, Osaka City University, Sumiyoshi-ku, Osaka 558, Japan, Department of Chemistry, Faculty of Education, Mie University, Tsu-shi, Mie 514, Japan, and Department of Chemistry, Faculty of Science, Hokkaido University, Kita-ku, Sapporo 060, Japan

Received April 24, 1996[⊗]

[$RuCl_2$(dmso)$_4$] (dmso = dimethyl sulfoxide) was treated with dhptaH_5 (1,3-diamino-2-hydroxypropanetetraacetic acid) and carboxylate ligands in the presence of NaOH or KOH and gave dinuclear ruthenium(III) complexes of dhpta with two bridging carboxylates, M[Ru(dhpta)(μ-$O_2CR)_2$] (**1**, R = C_6H_5, M = Na; **1′**, R = C_6H_5, M = K; **2**, R = *p*-OHC_6H_4, M = Na; **3**, R = *p*-$NH_2C_6H_4$, M = Na; **4**, R = CH_3, M = Na; **4′**, R = CH_3, M = K), which were characterized by elemental analysis, mass, electronic absorption, and ^{1}H and ^{13}C NMR spectroscopies, and X-ray absorption and crystallographic analyses (**4**, orthorhombic, space group $Pca2_1$ with a = 21.359(4) Å, b = 7.484(2) Å, c = 12.930(2) Å, Z = 4, R = 0.065, and R_w = 0.044 for 1116 independent reflections with $I > 3\sigma(I)$; **4′**·1.5H_2O: monoclinic, $P2_1$, a = 7.689(2) Å, b = 17.213(2) Å, c = 18.103(2) Å, β = 94.50(1) °, Z = 4, R = 0.041, and R_w = 0.047 for 4705 independent reflections with $I > 3\sigma(I)$). The complex anion consists of two ruthenium atoms bridged by the alkoxide of dhpta and the two acetate ligands. The Ru−Ru distances of 3.433(3) Å (**4**) and 3.421(1) Å (average) (**4′**) are longer than those found in (μ-oxo)bis(μ-carboxylato)diruthenium(III) complexes. EXAFS analysis and ^{1}H NMR spectra indicated that complexes **1**−**4** have the identical dinuclear structure in both solid and water solution states. Temperature-dependent magnetic susceptibility of **1**−**4** showed a strong antiferromagnetic interaction between the two Ru(III) ions with $-J$ = 310−470 cm^{-1}. Cyclic voltammograms showed two reduction processes at ca. −0.34 and ca. −0.94 V *vs* Ag/AgCl, corresponding to two stepwise one-electron reductions, $Ru^{III}Ru^{III} \leftrightarrow Ru^{III}Ru^{II} \leftrightarrow Ru^{II}Ru^{II}$. The most remarkable feature is the large separation between the two redox potentials, implying that the mixed-valence diruthenium(III,II) complexes of dhpta are fairly stable. Potentiostatic electrolysis of **1**−**4** at a potential in between $E^1_{1/2}$ and $E^2_{1/2}$ consumed 1 F per dimer and afforded a mixed-valence diruthenium species, [$Ru^{II}Ru^{III}$(dhpta)(μ-$O_2CR)_2$]$^{2-}$, in solution, which showed two weak and broad absorption bands (ν_{max} 5.5−5.7 and 11.6−11.9 kcm^{-1}) in DMF assignable to intervalence charge transfer (IT) bands. The lower energy IT band was analyzed by Gaussian curve fitting and the electron exchange integral H_{ad} was estimated as 640−870 cm^{-1} on the basis of Hush's theory. The spectroscopic analysis indicated that [$Ru^{II}Ru^{III}$(dhpta)($O_2CR)_2$]$^{2-}$ belongs to Class II type mixed-valence diruthenium complexes.

Introduction

Increasing attention has been focused on the chemistry of non-heme diiron proteins, including hemerythrin, ribonucleotide reductase, and methane monooxygenase, and their low molecular weight models of (μ-oxo)-, (μ-hydroxo)-, and (μ-alkoxo)diiron complexes have also been the subject of considerable investigation.[1] Whereas ruthenium ions are not involved in the active sites of metalloproteins, diruthenium centers have potential to provide redox chemistry parallel to that of diiron centers as well as catalytic organoreactions. In contrast with a wide variety of diiron model complexes,[1] the ruthenium analogues involving (μ-oxo)bis(μ-carboxylato)diruthenium and (μ-hydroxo)bis(μ-carboxylato)diruthenium cores have still been limited, and the (μ-alkoxo)bis(μ-carboxylato)diruthenium analogue has not been reported thus far. Wieghard and his co-workers have prepared [Ru^{III}_2(Me_3tacn)$_2$(μ-O)(μ-$O_2CR)_2$]$^{2+}$ (**5**), [Ru^{III}_2(Me_3tacn)$_2$(μ-OH)(μ-$O_2CR)_2$]$^{3+}$ (**6**), and [$Ru^{III}Ru^{IV}$(Me_3tacn)$_2$(μ-O)(μ-O_2-$CR)_2$]$^{3+}$ (**7**) by utilizing a face-capping ligand, 1,4,7-trimethyl-1,4,7-triazacyclononane ((Me_3tacn).[2ab] Their chemistry has recently extended to several mixed-metal dinuclear complexes containing a ruthenium atom.[2c] The similar (μ-oxo)bis(μ-carboxylato) complexes, [Ru^{III}_2(tmp)$_2$(μ-O)(μ-$O_2CCH_3)_2$]$^{2+}$ (**8**) (tmp = tris(1-pyrazolyl)methane),[3] and [Ru^{III}_2(py)$_6$(μ-O)(μ-O_2-$CCH_3)_2$]$^{2+}$ (**9**) (py = pyridine),[4] have also been reported, the

† Toho University.
‡ Nara Women's University.
§ Osaka University.
|| Osaka City.
⊥ Mie University.
& Hokkaido University.
⊗ Abstract published in *Advance ACS Abstracts,* September 1, 1996.

(1) (a) Lippard, S. J. *Angew. Chem. Int.Ed. Engl.* **1988**, *27*, 344. (b) Kurtz, D. M., Jr. *Chem. Rev.* **1990**, *90*, 585. (c) Feig, A.; Lippard, S. J. *Chem. Rev.* **1994**, *94*, 759.

(2) (a) Neubold, P.; Wieghardt, K.; Nuber, B.; Weiss, J. *Angew. Chem., Int. Ed. Engl.* **1988**, *27*, 933. (b) Neubold, P.; Wieghardt, K.; Nuber, B.; Weiss, J. *Inorg. Chem.* **1989**, *28*, 459. (c) Hotzelmann, R.; Wieghardt, K.; Ensling, J.; Romstedt, H.; Gutlich, P.; Bill, E.; Florke, U.; Haupt, H. J. *J. Am. Chem. Soc.* **1992**, *114*, 9470.

(3) Llobet, A.; Curry, M. E.; Evans, H. T.; Meyer, T. J. *Inorg. Chem.* **1989**, *28*, 3131.

S0020-1669(96)00435-1 CCC: $12.00

latter being characterized by X-ray crystallography. Chakravarty et al. have extensively carried out the study of carboxylate-bridged diruthenium complexes by using [$Ru_2Cl(\mu$-$O_2CR)_4$] as a precursor;[5] (μ-oxo)bis(μ-carboxylato) type complexes, [Ru^{III}_2-(μ-O)(μ-$O_2CAr)_2(MeCN)_4(PPh_3)_2]^{2+}$,[5a] [$Ru^{III}_2$($\mu$-O)($\mu$-$O_2CAr)_2$-$(NH_2CH_2CH_2NHC(Me)NH)_2(PPh_3)_2]^{2+}$,[5b] [$Ru^{III}_2$($\mu$-O)($\mu$-$O_2$-$CCH_3)_2(1\text{-MeIm})_6]^{2+}$ (1-MeIm = 1-methylimidazole),[5c] and [Ru^{III}_2(μ-O)(μ-$O_2CAr)_2(O_2CAr)(en)(PPh_3)_2]^{2+}$,[5d] and ($\mu$-alkoxo)-tris($\mu$-carboxylato) complexes, [Ru^{III}_2(μ-OMe)(μ-$O_2CAr)_3(1$-$MeIm)_4]^{2+}$,[5e] and (μ-aquo)bis(μ-carboxylato) complexes, [Ru^{II}-Ru^{III}(μ-OH_2)(μ-$O_2CAr)_2Cl(MeCN)(O_2CAr)_2(PPh_3)_2]$ and [Ru^{II}_2(μ-OH_2)(μ-$O_2CAr)_2(MeCN)_2(O_2CAr)_2(PPh_3)_2]$,[5f,g] have been prepared and structurally characterized. These carboxylate-bridged diruthenium cores showed interesting spectroscopic and redox properties.

Recently, we have initiated the diruthenium chemistry to elucidate structural and functional properties of dinuclear centers in connection with diiron centers included in biological systems. Here, we wish to report the synthesis and characterization of (μ-alkoxo)bis(μ-carboxylato)diruthenium complexes by using a dinucleating ligand, 1,3-diamino-2-hydroxypropanetetraacetic acid ($dhptaH_5$), together with their magnetic and electrochemical properties. Preliminary results have already been reported.[6]

Experimental Section

Materials. All reagents were of the best commercial grade and were used without further purification. [$RuCl_2$(dmso)$_4$] (dmso = dimethyl sulfoxide) was prepared by the known method.[7]

Measurements. ^{1}H and ^{13}C NMR spectra were measured on a JEOL GX-400 instrument at 400 and 100 MHz, respectively, in D_2O. ^{1}H−^{1}H and ^{1}H−^{13}C COSY spectra were recorded with the same instrument by using a PLUXS software. Infrared and electronic absorption spectra were recorded with Perkin-Elmer Model 1740 spectrometer and a Shimazu UV Model 3100 or 160 spectrometer, respectively. Mass spectra were measured on a JEOL DX300-JMA3100 spectrometer (FAB mode) by using an NBA matrix. Cyclic voltammograms were measured with a BASCV-50W voltammetric analyzer by using a conventional three electrode system, glassy carbon (working electrode), platinum wire (counter electrode), and Ag/AgCl (in H_2O) or Ag/$AgPF_6$ (in DMF) reference electrode. Potentiostatic electrolysis was carried out by a Nichiakeisoku NP-IR1000 potentiostat. Inductively coupled plasma-atomic emission spectroscopy (ICP) for Ru and Na was performed on a Shimazu ICPS-1000TR by using [$RuCl_2$(dmso)$_4$] and NaCl as references and H_2O/HNO_3 (1:1 v/v) as a solvent.

Magnetic susceptibility data were measured by the Faraday method over a range of 78−300 K with a Cahn 1000 RH electrobalance. Magnetic susceptibilities at room temperature were also obtained by the Gouy method. The diamagnetism of the complexes was corrected from Pascal's constants. The temperature dependence of the molar susceptibility was analyzed by using the van Vleck equation with the eigenvalues of the spin coupling Hamiltonian ($H = -2JS_1 \cdot S_2$, $S_1 = S_2 = {}^1/_2$). All data were fit to the van Vleck equation with a temperature-independent paramagnetism (TIP) term as shown in eq 1, where N = Avogadro's number, β = Bohr magneton, and k = Boltzman's constant.

$$\chi_m = \left(\frac{Ng^2\beta^2}{3kT}\right)\frac{1}{1+\frac{1}{3}\exp\left(\frac{-2J}{kT}\right)} + \mathrm{TIP} \qquad (1)$$

Preparation of M[Ru_2(dhpta)(μ-$O_2CC_6H_5)_2$] (1·4H_2O, M = Na; 1′·3H_2O, M = K). [$RuCl_2$(dmso)$_4$] (698 g, 1.44 mmol) was treated with $dhptaH_5$ (232 mg, 0.72 mmol) in water (20 mL) at 85 °C for 6 h. The solution was kept to pH 5 by 1.0 M sodium hydroxide. Then, a water suspension (10 mL) of $C_6H_5CO_2H$ (366 mg, 3 mmol), adjusted pH 5 by NaOH, was added to the reaction solution. The mixture was incubated at 85−90 °C for 16 h (monitored by electronic absorption spectra at 492 nm) and was chromatographed on a gel permeation column (Sephadex G-15, 4 cm × 30 cm) eluted with water. The reddish violet fraction was collected and concentrated to ca. 20 mL. An addition of ethanol to the solution gave crystals formulated as Na-[Ru_2(dhpta)(μ-$O_2CC_6H_5)_2$]·4H_2O (**1**·4H_2O) in 25% yield (152 mg), which were collected, washed with ethanol and diethyl ether, and dried in vacuo. Anal. Calcd for $C_{25}H_{23}N_2O_{13}Ru_2Na$·4$H_2O$: C, 35.05; H, 3.65; N. 3.27; Ru, 23.59; Na, 2.68. Found: C, 34.78; H, 3.51; N, 3.23; Ru, 24.12; N, 2.82. UV−vis (in H_2O): λ_{max} (ϵ) 495 (2.2 × 10^3), 373 (2.7 × 10^3), 234 (3.3 × 10^4) nm (M^{-1} cm^{-1}). FAB MS: m/e = 786 (M^+). K[Ru_2(dhpta)(μ-$O_2CC_6H_5)_2$]·3H_2O (**1′**·3H_2O) was obtained in 54% yield by a procedure similar to that described above, KOH being used instead of NaOH. Anal. Calcd for $C_{25}H_{23}N_2O_{13}Ru_2K$·3$H_2O$: C, 35.13; H, 3.42; N. 3.28. Found: C, 35.08; H, 3.60; N, 2.80.

Preparation of Na[Ru_2(dhpta){μ-O_2C(*p*-OHC_6H_4)}$_2$]·3H_2O (2·3H_2O). [$RuCl_2$(dmso)$_4$] (2.425 g, 5.0 mmol) was treated with $dhptaH_5$ (805 mg, 2.5 mmol) in water (50 mL) at 85 °C for 6 h. The solution was kept to pH 5 by 1.0 M sodium hydroxide. A water suspension (20 mL) of *p*-$OHC_6H_5CO_2H$ (1381 mg, 10 mmol), adjusted pH 5 by NaOH, was added to the reaction solution. The mixture was incubated at 85−90 °C for 36 h (monitored by electronic absorption spectra at 492 nm), and was chromatographed on a gel permeation column (Sephadex G-15, 4 cm × 30 cm) eluted with water. The reddish violet fraction was collected and concentrated to give crystals formulated as Na[Ru_2(dhpta){μ-O_2C(*p*-OHC_6H_4)}$_2$]·3H_2O (**2**·3H_2O) in 26% yield (575 mg), which were collected, washed with acetone and diethyl ether, and dried in vacuo. Anal. Calcd for $C_{25}H_{23}N_2O_{15}Ru_2Na$·3$H_2O$: C, 34.49; H, 3.35; N. 3.22. Found: C, 34.69; H, 3.87; N, 3.18. UV−vis (in H_2O): λ_{max} (ϵ) 494 (2.0 × 10^3), 370 (3.1 × 10^3), 260 (3.9 × 10^4) nm (M^{-1} cm^{-1}). FAB MS: m/e = 817 (M^+).

Preparation of Na[Ru_2(dhpta){μ-O_2C(*p*-$NH_2C_6H_4$)}$_2$]·5H_2O (3·5H_2O). [$RuCl_2$(dmso)$_4$] (2.425 g, 5.0 mmol) was treated with $dhptaH_5$ (805 mg, 2.5 mmol) in water (50 mL) at 85 °C for 6 h. The solution was kept to pH 5 by 1.0 M sodium hydroxide. Then, a water suspension (20 mL) of *p*-$NH_2C_6H_5CO_2H$ (1371 mg, 10 mmol), adjusted to pH 5 with NaOH, was added to the reaction solution. The mixture was incubated at 85−90 °C for 34 h (monitored by electronic absorption spectra at 495 nm) and was chromatographed on a gel permeation column (Sephadex G-15, 4 cm × 30 cm) eluted with water. The dark red fraction was collected and concentrated to ca. 20 mL, and an addition of ethanol and diethyl ether gave reddish violet crystals formulated as Na[Ru_2(dhpta){μ-O_2C(*p*-$NH_2C_6H_4$)}$_2$]·5H_2O (**3**·5H_2O) in 9% yield (194 mg), which were collected, washed with acetone and diethyl ether, and dried in vacuo. Anal. Calcd for $C_{25}H_{25}$-$N_4O_{13}Ru_2Na$·5H_2O: C, 33.19; H, 3.90; N. 6.19. Found: C, 33.57; H, 4.37; N, 6.11. UV−vis (in H_2O): λ_{max} (ϵ) 495 (1.9 × 10^3), 288 (4.3 × 10^4) nm (M^{-1} cm^{-1}). FAB MS: m/e = 816 (M^+).

Preparation of M[Ru_2(dhpta)(μ-$O_2CCH_3)_2$] (4, M = Na; 4′, M = K). [$RuCl_2$(dmso)$_4$] (2.425 g, 5.0 mmol) was treated with $dhptaH_5$ (805 mg, 2.5 mmol) in water (50 mL) at 85 °C for 6 h. The solution was kept to pH 5 by 1.0 M sodium hydroxide. A water solution (20 mL) of CH_3CO_2Na (4.1 g, 50 mmol), adjusted to pH 4−5 with acetic acid, was added to the reaction solution. The mixture was incubated at 85−90 °C for 12 h, and then a portion of CH_3CO_2Na (5.3 g, 65 mmol) was added to the reaction mixture. The solution was further incubated at 90 °C for 5 h at pH ∼4. The resultant solution was allowed to stand at room temperature to afford violet powder, which was recrystallized from a minimum amount of hot water (85 °C). Dark reddish violet crystals formulated as Na[Ru_2(dhpta)(μ-$O_2CCH_3)_2$] (**4**) were obtained in 40% yield (658 mg). Anal. Calcd for $C_{15}H_{19}N_2O_{13}$-Ru_2Na: C, 27.28; H, 2.90; N. 4.24. Found: C, 27.03; H, 2.96; N, 4.19. UV−vis (in H_2O): λ_{max} (ϵ) 490 (2.4 × 10^3), 370 (3.3 × 10^3), 269 (7.2 × 10^3) nm (M^{-1} cm^{-1}). K[Ru_2(dhpta)(μ-$O_2CCH_3)_2$] (**4′**) was

(4) Sasaki, Y.; Suzuki, M.; Tokiwa, A.; Ebihara, M.; Yamaguchi, T.; Kabuto, C.; Ito, T. *J. Am. Chem. Soc.* **1988**, *110*, 6251.
(5) (a) Das, B. K.; Chakravarty, A. R. *Inorg. Chem.* **1990**, *29*, 2078. (b) Syamala, A.; Chakravarty, A. R. *Inorg. Chem.* **1991**, *30*, 4699. (c) Sudha, C.; Mandal, S. K.; Chakravarty, A. R. *Inorg. Chem.* **1993**, *32*, 3801. (d) Syamala, A.; Nethaji, M.; Chakravarty, A. R. *Inorg. Chim. Acta* **1995**, *229*, 33. (e) Sudha, C.; Mandal, S. K.; Chakravarty, A. R. *Inorg. Chem.* **1994**, *33*, 4878. (f) Das, B. K.; Chakravarty, A. R. *Inorg. Chem.* **1990**, *29*, 1783. (g) Das, B. K.; Chakravarty, A. R. *Inorg. Chem.* **1991**, *30*, 4978.
(6) Tanase, T.; Kato, M.; Yamada, Y.; Tanaka, K.; Lee, K.; Sugihara, Y.; Ichimura, A.; Kinoshita, I.; Haga. M.; Sasaki, Y.; Yamamoto, Y.; Nagano, T.; Yano, S. *Chem. Lett.* **1994**, 1853.
(7) Evans, I. P.; Spencer, A.; Wilkinson, G. *J. Chem. Soc., Dalton Trans.* **1973**, 206.

Table 1. Crystallographic and Experimental Data for $Na[Ru_2(dhpta)(\mu\text{-}O_2CCH_3)_2]$ (**4**) and $K[Ru_2(dhpta)(\mu\text{-}O_2CCH_3)_2]\cdot 1.5H_2O$ (**4′**·$1.5H_2O$)

	4	**4′**·$1.5H_2O$
formula	$C_{15}H_{19}N_2O_{13}Ru_2Na$	$C_{15}H_{22}N_2O_{14.5}Ru_2K$
fw	660.45	703.58
cryst syst	orthorhombic	monoclinic
space group	$Pca2_1$ (No. 29)	$P2_1$ (No. 4)
a, Å	21.359(4)	7.689(2)
b, Å	7.484(2)	17.213(2)
c, Å	12.930(2)	18.103(2)
β, deg		94.50(1)
V, Å^3	2067(2)	2388.6(6)
Z	4	4
scan method	$\omega-2\theta$	$\omega-2\theta$
scan speed, deg/min	4	16
T, °C	23	20
D_{calcd}, g cm^{-1}	2.122	1.956
abs coeff, cm^{-1}	15.24	15.12
trans factor	0.80−1.00	0.92−1.00
2θ range, deg	$3 < 2\theta < 50$	$3 < 2\theta < 55$
no. of unique data	2117	6077
no. of obsd data	1116 ($I > 3\sigma(I)$)	4705 ($I > 3\sigma(I)$)
no. of variables	148	622
R[a]	0.065	0.041
R_w[a]	0.044	0.047

[a] $R = \sum||F_o| - |F_c||/\sum|F_o|$; $R_w = [\sum w(|F_o| - |F_c|)^2/\sum w|F_o|^2]^{1/2}$ ($w = 1/\sigma^2(F_o)$).

obtained in 18% yield by a procedure similar to that described above, KOH and CH_3CO_2K being used instead of NaOH and CH_3CO_2Na, respectively. Anal. Calcd for $C_{15}H_{19}N_2O_{13}Ru_2K$: C, 26.63; H, 2.83; N. 4.14. Found: C, 26.77; H, 3.13; N, 3.98.

X-ray Crystallographic Analyses of $Na[Ru_2(dhpta)(\mu\text{-}O_2CCH_3)_2]$ (4) and $K[Ru_2(dhpta)(\mu\text{-}O_2CCH_3)_2]\cdot 1.5H_2O$ (4′·$1.5H_2O$). Suitable crystals for X-ray crystallography were obtained by recrystallizations of **4** and **4′** from a water/ethanol mixed solvent. Crystal data and experimental conditions are listed in Table 1. All data were collected on an Rigaku AFC5S (**4**) and AFC7R (**4′**) diffractometers by using graphite-monochromatized Mo Kα ($\lambda = 0.710\,69$ Å) radiation. Three standard reflections were monitored every 150 reflections and showed no systematic decrease in intensity. Reflection data were corrected for Lorentz−polarization and absorption (by ψ-scan method) effects.

The structure of **4** was solved by direct methods with MITHRIL.[8] The positions of two ruthenium atoms were determined by the initial E map, and subsequent Fourier and difference Fourier syntheses gave the positions of other non-hydrogen atoms. The coordinates of all hydrogen atoms were calculated at the ideal positions with the C−H distance of 0.95 Å, and were not refined. The structure was refined with the full-matrix least-square techniques minimizing $\sum w(|F_o| - |F_c|)^2$. Final refinement with anisotropic thermal parameters for the Ru and Na atoms and isotropic ones for other non-hydrogen atoms converged to $R = 0.065$ and $R_w = 0.044$ ($w = 1/\sigma^2(F_o)$). It should be noted that the crystal of **4** was obtained as a twin and was cut into two pieces along the *bc* plane, one of which was used in the data collection. This procedure may be responsible for somewhat poor reflection data, resulting in a low grade crystal structure of **4**. The structure of **4′**·$1.5H_2O$ was solved by direct methods (SHELXS86)[9] and Fourier syntheses, and was further refined with full-matrix least-square techniques. Two sets of $K[Ru_2(dhpta)(\mu\text{-}O_2CCH_3)_2]$ and three water molecules were determined independently in an asymmetric unit. The coordinates of all hydrogen atoms were calculated taking the C−H distance as 0.95 Å and were fixed in the refinement. Final refinement with anisotropic thermal parameters for non-hydrogen atoms converged to $R = 0.041$ and $R_w = 0.047$. Atomic scattering factors and f' and f'' for Ru, K, Na, O, N, and C were taken from the literature.[10] All calculations were carried out on a Digital VAX Station 3100 and a Silicon Graphics Indigo2 Station with the TEXSAN Program System.[11] Perspective drawings were drawn by using programs ORTEP[12] and PLUTO.[13] The final atomic coordinates for non-hydrogen atoms are listed in Table 2. Compilations of final atomic parameters for all atoms are supplied as Supporting Information.

EXAFS Analysis. X-ray absorption measurements around Ru K edge (21.568−23.118 keV with 780 steps) were performed at the Photon Factory of the National Laboratory for High Energy Physics on beam line 10B using synchrotron radiation (2.5 GeV, 340−300 mA). The experiments were done in the transmission mode on powdered and solution (in H_2O) samples using a Si(311) monochromator. The theoretical expression of the obtained $\boldsymbol{k}^3\chi(\boldsymbol{k})$ for the case of single scattering is shown in eq 2,[14] where $\boldsymbol{r}_i$, N_i, S_i, $F_i(\boldsymbol{k})$, $\Phi_i(\boldsymbol{k})$, and σ_i

$$\boldsymbol{k}^3\chi(\boldsymbol{k}) = \sum_i \left(\frac{\boldsymbol{k}^2 N_i}{\boldsymbol{r}_i^2} S_i F_i(\boldsymbol{k}) \exp(-2s_i^2\boldsymbol{k}^2) \sin(2\boldsymbol{k}\boldsymbol{r}_i + \Phi_i(\boldsymbol{k})) \right) \quad (2)$$

represent the interatomic distance, the coordination number, the reducing factor, the back-scattering amplitude, the phase shift, and the Debye−Waller factor, respectively, and $\boldsymbol{k}$ is the photoelectron wave vector defined as $\boldsymbol{k} = [(2m/\hbar^2)(E - E_0)]^{1/2}$ ($E_0 = 22.120$ keV). The back-scattering amplitude $F_i(\boldsymbol{k})$ and the phase shift $\Phi_i(\boldsymbol{k})$ functions used were the theoretical parameters tabulated by Teo and Lee[15] and the empirical parameters derived from the preanalysis of **4**. Parameters, N_i, $\boldsymbol{r}_i$, and σ_i were varied in the nonlinear least-squares refined curve fitting, and fixed values of S_i and E_0 were used. The E_0 was determined from the spectrum of complex **4** (powder) as a point (22119.5 eV) which has a maximum $d\mu/dE$ value. The fixed reducing factors S_i are determined by the analysis of **4** (powder) with $N_{N/O}$, N_C, and N_{Ru} fixed to 6, 6, and 1, respectively. The Fourier filtered method for each shell (Ru−N/O, Ru−C, and Ru−Ru) was applied to avoid strong parameter correlations. All calculations were performed on a HITAC M-680H at the Computer Center of the University of Tokyo with the systematic programs EXAFS1.[16]

Results and Discussion

Preparation of $M[Ru_2(dhpta)(\mu\text{-}O_2CR)_2]$ (M = Na, K). $[RuCl_2(dmso)_4]$ was treated with $dhptaH_5$ in water at 85 °C for 6 h. The solution was kept to pH 5 by 1.0 M sodium hydroxide or potassium hydroxide. Then, a water solution or suspension of carboxylic acid (adjusted pH 5 by NaOH) was added to the reaction solution. The mixture was incubated at 85−90 °C for 5−36 h (monitored by electronic absorption spectra at 492−495 nm). Purifications by chromatography on a gel permeation column (Sephadex G-15) and/or recrystallization afforded reddish violet crystals formulated as $M[Ru_2(dhpta)(\mu\text{-}O_2CR)_2]$ (**1**, R = C_6H_5, M = Na; **1′**, R = C_6H_5, M = K; **2**, R = *p*-OHC_6H_4, M = Na; **3**, R = *p*-$NH_2C_6H_4$, M = Na; **4**, R = CH_3, M = Na; **1**, R = CH_3, M = K) in 9−54% yields. Complexes **1**−**4** could also be prepared by an one-pot reaction of $[RuCl_2(dmso)_4]$ with $dphtaH_5$ and RCO_2H in a slightly acidic solution. The IR spectra of **1**−**4** were similar to each other and indicated the presence of carboxylate and dhpta ligands around 1645−1500 ($\nu_{as}(CO_2)$) and 1470−1325 ($\nu_{sym}(CO_2)$) cm^{-1}. In the electronic absorption spectra, a weak absorption

(8) Gilmore, G. J. *J. Appl. Crystallogr.* **1984**, *17*, 42.
(9) Sheldrick, G. M. *In Crystallography Computing*; Sheldrick, G. M., Krüger, C., Goddard, R., Eds.; Oxford University Press: Oxford, U.K., 1985; p 175.
(10) (a) Cromer, D. T. *Acta Crystallogr.* **1965**, *18*, 17. (b) Cromer, D. T.; Waber, J. T. *International Tables for X-ray Crystallography*; Kynoch Press: Birmingham, England, 1974; Vol. IV.
(11) *TEXSAN*; Molecular Structure Corporation: The Woodlands, TX, 1985 and 1992.
(12) Johnson, C. K. *ORTEP-II*; Oak Ridge National Laboratory: Oak Ridge, TN, 1976.
(13) Motherwell, S.; Clegg, W. PLUTO: Program for Ploting Molecuar and Crystal Structures. University of Cambridge, England, 1978.
(14) Sayers, D. E.; Stern, E. A.; Lytle, F. W. *Phys. Rev. Lett.* **1971**, *27*, 1204.
(15) (a) Teo, B. K.; Lee, P. A.; Simons, A. L.; Eisenberger, P.; Kincaid, B. M. *J. Am. Chem. Soc.* **1977**, *99*, 3854. (b) Teo, B. K.; Lee, P. A. *J. Am. Chem. Soc.* **1979**, *101*, 2815.
(16) Kosugi, N.; Kuroda, H. Program EXAFS1. Research Center for Spectrochemistry, University of Tokyo, Japan, 1985.

Table 2. Atomic Positional and Thermal Parameters for Non-Hydrogen Atoms of Na[Ru$_2$(dhpta)(μ-O$_2$CCH$_3$)$_2$] (**4**) and K[Ru$_2$(dhpta)(μ-O$_2$CCH$_3$)$_2$]·1.5H$_2$O (**4′**·1.5H$_2$O)[a–c]

	x	*y*	*z*	B_{eq}, Å^2		*x*	*y*	*z*	B_{eq}, Å^2
				Na[Ru$_2$(dhpta)(μ-O$_2$CCH$_3$)$_2$] (**4**)					
Ru(1)	0.4657(1)	0.4173(3)	0.3053	1.54(8)	N(2)	0.298(1)	0.284(3)	0.108(2)	1.9(5)
Ru(2)	0.3340(1)	0.1822(3)	0.2375(2)	1.60(9)	C(1)	0.550(1)	0.514(3)	0.140(2)	2.1(6)
Na(1)	0.6250(5)	0.081(2)	0.320(1)	3.4(5)	C(2)	0.581(1)	0.372(4)	0.198(2)	2.9(7)
O(1)	0.5428(8)	0.287(2)	0.265(1)	2.4(4)	C(3)	0.503(1)	0.762(3)	0.245(3)	3.1(7)
O(2)	0.6365(9)	0.340(3)	0.190(1)	3.5(5)	C(4)	0.532(1)	0.728(4)	0.354(2)	2.4(6)
O(3)	0.5180(8)	0.581(3)	0.399(1)	2.3(4)	C(5)	0.303(1)	0.148(4)	0.023(2)	2.1(6)
O(4)	0.5638(9)	0.850(3)	0.394(1)	3.7(5)	C(6)	0.337(1)	−0.021(3)	0.054(2)	1.7(5)
O(5)	0.3510(7)	−0.030(2)	0.152(1)	1.1(3)	C(7)	0.231(1)	0.322(4)	0.132(2)	1.6(5)
O(6)	0.3424(8)	−0.140(2)	−0.008(1)	2.2(4)	C(8)	0.207(1)	0.174(4)	0.202(2)	2.9(6)
O(7)	0.2439(7)	0.093(2)	0.262(1)	2.3(4)	C(9)	0.436(1)	0.603(4)	0.124(2)	1.7(5)
O(8)	0.1472(8)	0.145(3)	0.205(1)	2.6(5)	C(10)	0.402(1)	0.423(4)	0.106(2)	1.6(5)
O(9)	0.4089(7)	0.320(2)	0.204(1)	1.0(3)	C(11)	0.334(1)	0.456(3)	0.086(2)	1.1(5)
O(11)	0.4497(8)	0.231(2)	0.424(1)	1.9(4)	C(21)	0.328(1)	0.530(3)	0.359(2)	1.5(5)
O(12)	0.3693(8)	0.046(2)	0.368(1)	2.0(4)	C(22)	0.297(1)	0.673(5)	0.412(2)	3.7(7)
O(21)	0.3903(9)	0.565(3)	0.357(1)	3.2(5)	C(31)	0.416(1)	0.091(4)	0.430(2)	1.8(5)
O(22)	0.3088(8)	0.394(3)	0.328(1)	3.4(5)	C(32)	0.432(1)	−0.035(3)	0.511(2)	1.3(5)
N(1)	0.4885(9)	0.590(3)	0.198(1)	1.6(4)					
				K[Ru$_2$(dhpta)(μ-O$_2$CCH$_3$)$_2$]·1.5H$_2$O (**4′**·1.5H$_2$O)					
Ru(1)	−0.2410(1)	0.4115	0.19358(5)	2.17(2)	N(1)	−0.317(1)	0.4956(6)	0.2620(5)	2.0(2)
Ru(2)	−0.4996(1)	0.4138(1)	0.03096(5)	2.39(2)	N(2)	−0.676(1)	0.5021(7)	0.0311(6)	3.0(2)
Ru(3)	1.2054(1)	0.13130(8)	0.49077(5)	1.71(2)	N(3)	1.110(1)	0.2376(5)	0.5154(5)	1.9(2)
Ru(4)	0.9275(1)	0.04062(8)	0.36150(5)	1.86(2)	N(4)	0.742(1)	0.1151(6)	0.3186(5)	2.1(2)
K(1)	0.2809(5)	0.3302(2)	0.7899(2)	3.99(8)	C(1)	−0.178(1)	0.5573(7)	0.2676(7)	2.5(3)
K(2)	0.7910(3)	0.4589(2)	0.8284(2)	2.97(6)	C(2)	−0.027(2)	0.5395(9)	0.2246(7)	2.9(3)
O(1)	−0.034(1)	0.4800(6)	0.1843(5)	2.8(2)	C(3)	−0.327(2)	0.4573(8)	0.3347(6)	2.6(3)
O(2)	0.095(1)	0.5867(7)	0.2286(6)	5.0(3)	C(4)	−0.174(2)	0.4014(8)	0.3469(7)	2.7(3)
O(3)	−0.129(1)	0.3651(5)	0.2889(5)	3.1(2)	C(5)	−0.622(2)	0.569(1)	−0.0205(7)	3.8(3)
O(4)	−0.107(1)	0.3923(6)	0.4094(5)	3.8(2)	C(6)	−0.471(2)	0.543(1)	−0.0662(7)	3.3(3)
O(5)	−0.389(1)	0.4780(6)	−0.0450(5)	3.4(2)	C(7)	−0.845(2)	0.4666(9)	0.0039(7)	3.3(3)
O(6)	−0.436(1)	0.5793(7)	−0.1168(6)	5.0(3)	C(8)	−0.819(2)	0.403(1)	−0.0539(7)	3.1(3)
O(7)	−0.670(1)	0.3679(6)	−0.0492(5)	3.1(2)	C(9)	−0.489(2)	0.5232(7)	0.2281(7)	2.5(3)
O(8)	−0.938(1)	0.3865(6)	−0.1001(5)	4.1(3)	C(10)	−0.485(1)	0.5318(8)	0.1439(6)	2.4(2)
O(9)	−0.384(1)	0.4660(5)	0.1164(4)	2.4(2)	C(11)	−0.671(2)	0.5300(9)	0.1083(6)	3.0(3)
O(10)	−0.448(1)	0.3402(6)	0.2066(5)	3.1(2)	C(12)	−0.582(2)	0.3210(7)	0.1666(7)	2.6(3)
O(11)	−0.627(1)	0.3443(6)	0.1030(5)	3.3(2)	C(13)	−0.713(2)	0.268(1)	0.2000(8)	4.5(4)
O(12)	−0.141(1)	0.3272(6)	0.1255(5)	3.3(2)	C(14)	−0.186(2)	0.3050(7)	0.0620(7)	2.6(3)
O(13)	−0.317(1)	0.3261(6)	0.0200(5)	3.2(2)	C(15)	−0.067(2)	0.2452(8)	0.0316(8)	3.5(3)
O(14)	1.380(1)	0.1917(5)	0.4397(5)	2.4(2)	C(16)	1.217(2)	0.2977(7)	0.4810(7)	2.5(3)
O(15)	1.444(1)	0.3100(6)	0.4034(6)	4.4(3)	C(17)	1.356(2)	0.2652(7)	0.4373(7)	2.5(3)
O(16)	1.348(1)	0.1455(5)	0.5901(4)	2.4(2)	C(18)	1.128(1)	0.2461(7)	0.5952(7)	2.2(2)
O(17)	1.370(1)	0.2275(6)	0.6856(5)	3.3(2)	C(19)	1.294(2)	0.2058(8)	0.6267(6)	2.6(3)
O(18)	1.023(1)	0.0509(6)	0.2636(4)	2.7(2)	C(20)	0.792(2)	0.1419(8)	0.2451(6)	2.9(3)
O(19)	0.950(1)	0.0923(6)	0.1488(5)	4.1(3)	C(21)	0.929(2)	0.0926(8)	0.2135(7)	2.7(3)
O(20)	0.762(1)	−0.0426(5)	0.3186(5)	2.8(2)	C(22)	0.575(2)	0.0698(8)	0.3126(7)	2.9(3)
O(21)	0.498(1)	−0.0538(6)	0.2608(5)	3.8(2)	C(23)	0.613(2)	−0.0159(8)	0.2938(7)	2.6(3)
O(22)	1.0369(9)	0.1339(5)	0.4047(4)	1.8(1)	C(24)	0.927(1)	0.2363(7)	0.4827(7)	2.4(3)
O(23)	1.018(1)	0.0738(5)	0.5484(4)	2.1(2)	C(25)	0.927(1)	0.2048(8)	0.4025(7)	2.4(3)
O(24)	0.820(1)	0.0245(5)	0.4611(4)	2.6(2)	C(26)	0.739(2)	0.1826(7)	0.3746(7)	2.6(3)
O(25)	1.320(1)	0.0257(5)	0.4667(5)	2.5(2)	C(27)	0.875(1)	0.0413(8)	0.5281(6)	2.1(2)
O(26)	1.120(1)	−0.0410(5)	0.3948(4)	2.6(2)	C(28)	0.759(2)	0.0177(9)	0.5850(7)	3.4(3)
O(27)	−0.072(1)	0.3490(6)	0.7275(5)	3.7(2)	C(29)	1.264(1)	−0.0340(7)	0.4336(6)	2.2(2)
O(28)	0.630(2)	0.291(1)	0.8613(8)	11.8(7)	C(30)	1.383(2)	−0.1035(8)	0.4365(7)	2.9(3)
O(29)	1.745(2)	0.2155(8)	0.705(1)	9.8(5)					

[a] Estimated standard deviations are given in parentheses. [b] The Ru and Na atoms of **4** and all atoms of **4′**·1.5H$_2$O were refined with anisotropic thermal parameters given as the isotropic equivalent displacement parameter defined as $B_{eq} = (8\pi^2/3)(U_{11}(aa^*)^2 + U_{22}(bb^*)^2 + U_{33}(cc^*)^2 + 2U_{12}aa^*bb^*\cos\gamma + 2U_{13}aa^*cc^*\cos\beta + 2U_{23}bb^*cc^*\cos\alpha)$. [c] The O, N, and C atoms of **4** were refined isotropically.

band, similar to that of (μ-hydroxo)bis(μ-carboxylato)diruthenium complex, [Ru$^{III}_2$(Me$_3$tacn)$_2$(μ-OH)(μ-O$_2$CR)$_2$]$^{3+}$ (**6**),[2a,b] was observed around 490 nm with ϵ = 1900−2400 M^{-1} cm^{-1} (Figure 1). The intense absorptions at 230−290 nm (ϵ 33 × 10^3 to 43 × 10^3 M^{-1} cm^{-1}) for **1**−**3** are derived from the phenyl groups of carboxylates. The FAB mass spectra of **1**−**3** indicated a diruthenium structure with one dhpta and two carboxylate ligands together with a sodium countercation, whereas that of **4** did not show the peak corresponding to Na[Ru$_2$(dhpta)(μ-O$_2$CCH$_3$)$_2$]. The parent peaks for **1**−**3**, the centers of which correspond to the moleculer weights of Na[Ru$_2$(dhpta)(μ-O$_2$CR)$_2$], exhibited very complicated spectral patterns owing to a pair of Ru atoms having a wide variety of isotope distribution over ^{96}Ru−^{104}Ru. The calculated and observed MS spectra of **2** and **3** (the parent peak region corresponding to Na[Ru$_2$(dhpta)(μ-O$_2$CC$_6$H$_4$R)$_2$]) are shown in Figure 2.

X-ray Crystallographic Analyses of Na[Ru$_2$(dhpta)(μ-O$_2$CCH$_3$)$_2$] (4) and K[Ru$_2$(dhpta)(μ-O$_2$CCH$_3$)$_2$]·1.5H$_2$O (4′·1.5H$_2$O). The structures of M[Ru$_2$(dhpta)(μ-O$_2$CCH$_3$)$_2$] (**4**: M = Na, **4′**: M = K) were determined by X-ray crystallography. The asymmetric unit of **4′**·1.5H$_2$O involves two crystallographically independent complex anions, [Ru$_2$(dhpta)(μ-O$_2$CCH$_3$)$_2$]$^-$, two potassium cations, and three solvent water molecules. The structures of the two complex anions, A and B, are almost identical, perspective drawings with the atomic numbering scheme being illustrated in Figure 3. Some selected

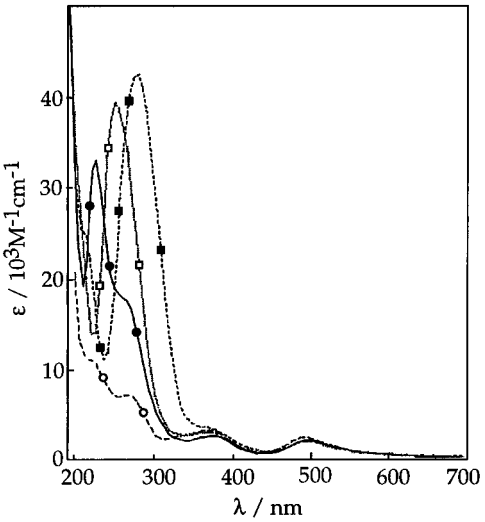

Figure 1. Electronic absorption spectra of (a) $Na[Ru_2(dhpta)(\mu\text{-}O_2CC_6H_5)_2]$ (**1**) (●), (b) $Na[Ru_2(dhpta)(\mu\text{-}O_2C(p\text{-}OHC_6H_4))_2]$ (**2**) (□), (c) $Na[Ru_2(dhpta)(\mu\text{-}O_2C(p\text{-}NH_2C_6H_4))_2]$ **3** (■), and (d) $Na[Ru_2(dhpta)(\mu\text{-}O_2CCH_3)_2]$ (**4**) (○) in H_2O.

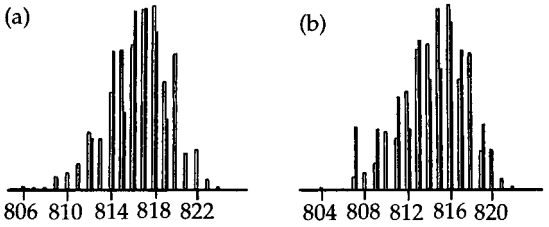

Figure 2. FAB mass spectra of (a) **2** and (b) **3** in the M^+ region. Black and white bars represent observed and calculated peaks, respectively.

bond lengths and angles are listed in Table 3. The complex anion consists of two ruthenium atoms symmetrically bridged by the alkoxide of dhpta and the two acetate ligands to give a confacial bioctahedral structure, which is similar to that found in $(Me_4N)[Fe_2L(\mu\text{-}O_2CCH_3)_2]$ (L = *N*,*N*′-(2-hydroxy-5-methyl-1,3-xylylene)bis(N-carboxymethylglycine)).[17] The each Ru atom shows a slightly distorted octahedral geometry with the smallest *trans* and *cis* angles of 166.7(3)° (O(20)−Ru(4)−O(22) in B) and 83.0(3)° (O(16)−Ru(3)−N(3) in B), respectively. The Ru−Ru distances of 3.421(1) Å (A) and 3.420(1) Å (B) are out of the range for the Ru−Ru single bond which was observed in (*μ*-hydroxo)diruthenium(III) complexes, $[Ru_2(Me_3tacn)_2(\mu\text{-}OH)_2(\mu\text{-}O_2CCH_3)]^{3+}$ (2.572(3) Å)[18] and $[Ru_2(Me_3tacn)_2(\mu\text{-}OH)_3]^{3+}$ (2.505(3) Å),[19] and are longer by ca. 0.18 Å than those found in (*μ*-oxo)bis(*μ*-carboxylato)diruthenium(III) complexes, **5** (3.258(1) Å, R = CH_3) **9** (3.251(2) Å), and $[Ru_2(\mu\text{-}O)(\mu\text{-}O_2CC_6H_5)_2(PPh_3)_2(MeCN)_4]^{2+}$ (**10**) (3.237(1) Å).[5a] The long Ru−Ru distance is mainly ascribable to longer bond distances between the ruthenium and the *μ*-alkoxo oxygen atom (1.943(8)−1.949(8) Å, average 1.947 Å) than those between the ruthenium and the *μ*-oxo oxygen atoms in **5**, **9**, and **10** (1.857−1.884 Å). The $Ru-O_{alkoxo}-Ru$ bent angles are 123.0(5) and 122.8(4)° (average 122.9°). The two bridging acetates are almost coplanar with the Ru_2O_2 planes.

The K^+ countercations are well packed between the column of complex anions in the lattice, resulting in an infinite chain

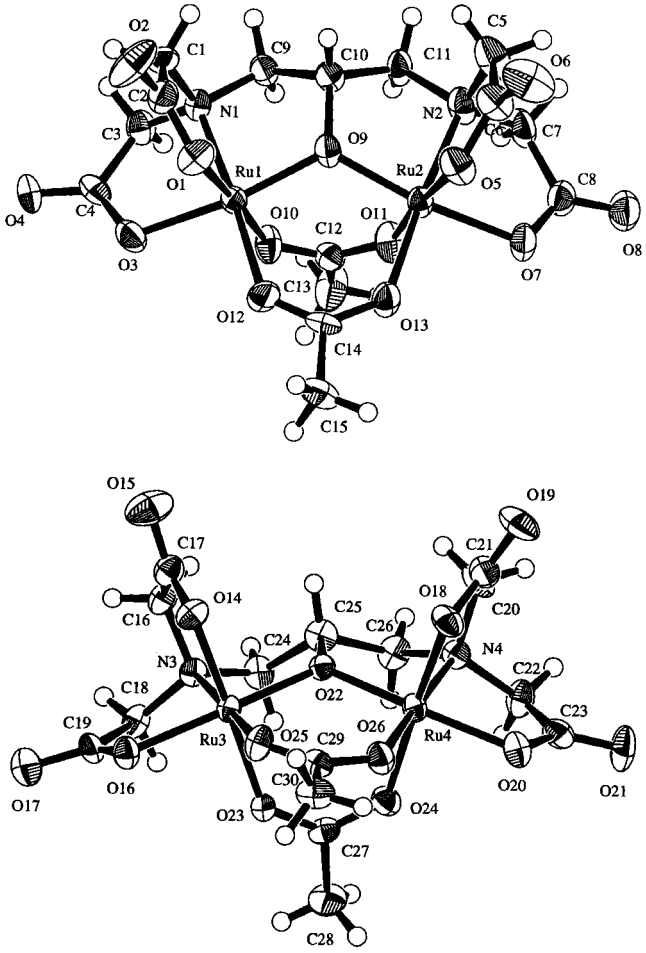

Figure 3. ORTEP plots of the complex anions of $K[Ru_2(dhpta)(\mu\text{-}O_2CCH_3)_2]$ (**4′**); (a) anion A and (b) anion B.

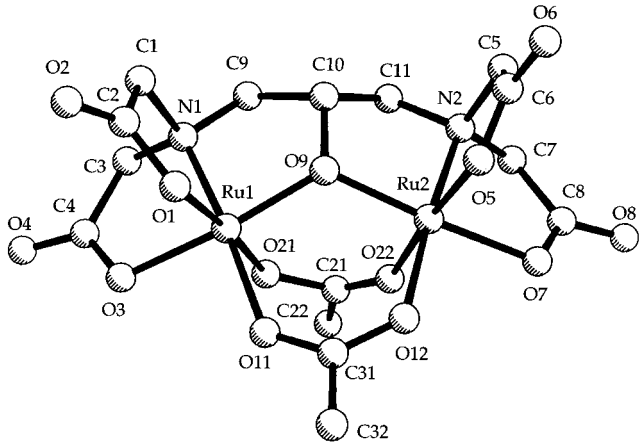

Figure 4. PLUTO diagram of the complex anion of $Na[Ru_2(dhpta)(\mu\text{-}O_2CCH_3)_2]$ (**4**).

aggregation (K(1)···K(2) = 4.511(5) Å, K(1)···K(2)* = 4.472(4) Å) joined by the carbonyl oxygen atoms of the dhpta acetate arms (K−O = 2.653(9)−3.05(1) Å) and the water molecules (O(27), O(28) of crystallization (K−O = 2.653(9)−3.22(2) Å).

The structure of the complex anion of **4** is essentially identical to that of **4′**, demonstrating that the countercations do not affect the diruthenium core (Figure 4 and Table 4). The Ru···Ru interatomic distance is 3.433(3) Å, and the $Ru-O_{alkoxo}-Ru$ angle is 124.1(7)°. The average $Ru-O_{alkoxo}$ and $Ru-O_{acetate}$ bond lengths are 1.94 and 2.08 Å, respectively. The counter-

(17) Murch, B. P.; Bradley, F. C.; Que, L., Jr. *J. Am. Chem. Soc*. **1986**, *108*, 5027.
(18) Wieghardt, K.; Herrmann, W.; Koppen, M. *Z. Naturforsch.* **1984**, *39B*, 1335.
(19) Neubold, R.; Vedova, B. S. P. C. D.; Wieghardt, K.; Nuber, B.; Weiss, J. *Inorg. Chem.* **1990**, *29*, 2078.

Table 3. Selected Bond Distances (Å) and Angles (deg) for K[Ru$_2$(dhpta)(μ-O$_2$CCH$_3$)$_2$]·1.5H$_2$O (**4′**·1.5H$_2$O)[a]

Bond Distances			
Ru(1)···Ru(2)	3.421(1)	Ru(2)···Ru(3)	3.420(1)
Ru(1)−O(1)	1.997(8)	Ru(1)−O(3)	2.030(8)
Ru(1)−O(9)	1.949(8)	Ru(1)−O(10)	2.037(9)
Ru(1)−O(12)	2.089(9)	Ru(1)−N(1)	2.02(1)
Ru(2)−O(5)	2.004(9)	Ru(2)−O(7)	2.039(8)
Ru(2)−O(9)	1.943(8)	Ru(2)−O(11)	2.073(9)
Ru(2)−O(13)	2.084(9)	Ru(2)−N(2)	2.04(1)
Ru(3)−O(14)	1.982(8)	Ru(3)−O(16)	2.047(7)
Ru(3)−O(22)	1.946(7)	Ru(3)−O(23)	2.090(8)
Ru(3)−O(25)	2.082(8)	Ru(3)−N(3)	2.033(9)
Ru(4)−O(18)	1.978(8)	Ru(4)−O(20)	2.031(9)
Ru(4)−O(22)	1.949(8)	Ru(4)−O(24)	2.059(8)
Ru(4)−O(26)	2.094(8)	Ru(4)−N(4)	2.029(9)
Bond Angles			
O(1)−Ru(1)−O(3)	91.0(4)	O(1)−Ru(1)−O(9)	93.6(4)
O(1)−Ru(1)−O(10)	177.9(4)	O(1)−Ru(1)−O(12)	91.6(4)
O(1)−Ru(1)−N(1)	84.1(4)	O(3)−Ru(1)−O(9)	167.4(3)
O(3)−Ru(1)−O(10)	86.9(4)	O(3)−Ru(1)−O(12)	94.4(4)
O(3)−Ru(1)−N(1)	83.3(4)	O(9)−Ru(1)−O(10)	88.4(3)
O(9)−Ru(1)−O(12)	97.2(3)	O(9)−Ru(1)−N(1)	85.4(4)
O(10)−Ru(1)−O(12)	88.7(4)	O(10)−Ru(1)−N(1)	95.5(4)
O(12)−Ru(1)−N(1)	175.1(3)	O(5)−Ru(2)−O(7)	90.6(4)
O(5)−Ru(2)−O(9)	95.7(4)	O(5)−Ru(2)−O(11)	175.6(4)
O(5)−Ru(2)−O(13)	90.5(4)	O(5)−Ru(2)−N(2)	84.7(4)
O(7)−Ru(2)−O(9)	167.1(3)	O(7)−Ru(2)−O(11)	85.0(4)
O(7)−Ru(2)−O(13)	93.0(3)	O(7)−Ru(2)−N(2)	84.2(4)
O(9)−Ru(2)−O(11)	88.6(4)	O(9)−Ru(2)−O(13)	98.1(3)
O(9)−Ru(2)−N(2)	85.3(4)	O(11)−Ru(2)−O(13)	89.9(4)
O(11)−Ru(2)−N(2)	94.7(4)	O(13)−Ru(2)−N(2)	174.4(4)
O(14)−Ru(3)−O(16)	90.6(3)	O(14)−Ru(3)−O(22)	92.7(3)
O(14)−Ru(3)−O(23)	176.4(3)	O(14)−Ru(3)−O(25)	92.7(3)
O(14)−Ru(3)−N(3)	84.2(4)	O(16)−Ru(3)−O(22)	167.9(3)
O(16)−Ru(3)−O(23)	87.8(3)	O(16)−Ru(3)−O(25)	94.7(3)
O(16)−Ru(3)−N(3)	83.0(3)	O(22)−Ru(3)−O(23)	88.2(3)
O(22)−Ru(3)−O(25)	96.8(3)	O(22)−Ru(3)−N(3)	85.8(4)
O(23)−Ru(3)−O(25)	90.6(3)	O(23)−Ru(3)−N(3)	92.5(3)
O(25)−Ru(3)−N(3)	176.0(3)	O(18)−Ru(4)−O(20)	89.2(4)
O(18)−Ru(4)−O(22)	96.2(3)	O(18)−Ru(4)−O(24)	176.7(4)
O(18)−Ru(4)−O(26)	90.8(3)	O(18)−Ru(4)−N(4)	84.2(4)
O(20)−Ru(4)−O(22)	166.7(3)	O(20)−Ru(4)−O(24)	87.5(3)
O(20)−Ru(4)−O(26)	92.6(3)	O(20)−Ru(4)−N(4)	84.1(4)
O(22)−Ru(4)−O(24)	87.1(3)	O(22)−Ru(4)−O(26)	99.5(3)
O(22)−Ru(4)−N(4)	84.4(4)	O(24)−Ru(4)−O(26)	88.9(3)
O(24)−Ru(4)−N(4)	95.8(4)	O(26)−Ru(4)−N(4)	174.1(4)
Ru(1)−O(9)−Ru(2)	123.0(5)	Ru(3)−O(22)−Ru(4)	122.8(4)
Ru(1)−O(10)−C(12)	134.8(9)	Ru(2)−O(11)−C(12)	131.2(9)
Ru(1)−O(12)−C(14)	132.4(8)	Ru(2)−O(13)−C(14)	131.4(8)
Ru(3)−O(23)−C(27)	133.1(7)	Ru(4)−O(24)−C(27)	132.1(7)
Ru(3)−O(25)−C(29)	133.0(7)	Ru(4)−O(26)−C(29)	131.3(8)

[a] Estimated standard deviations are given in parentheses. See Figure 3 for atom labels.

cation Na$^+$ is ligated by six carbonyl oxygen atoms of the dhpta acetate arms in the crystal packing (Na−O = 2.30(2)−2.95(2) Å).

EXAFS Analyses. In order to elucidate the influence of μ-carboxylate groups on the diruthenium structure, EXAFS (extended X-ray absorption fine structure) analyses were carried out on complexes **1**−**4**. The Fourier transform of the EXAFS data for **4** in both solid and solution states are shown in Figure 5a, showing no structural change around the dinuclear core on dissolution in water. Three peaks were observed at about 1.6, 2.4, and 3.1 Å (before phase-shift correction), which were assigned to the back-scattering contributions of the nitrogen and oxygen atoms (N/O) coordinating to the ruthenium, the carbon atoms (C) including five-membered chelate rings, and the outer ruthenium atom (Ru), respectively, by curve-fitting analyses. The N and O atoms involved in the first coordination sphere were not able to be distinguished in the present analyses. The Fourier filtered technique was applied in the curve-fitting for each peak to avoid strong parameter correlations in the case of three terms fit with $\boldsymbol{k}^3\chi(\boldsymbol{k})_{\mathrm{calcd}} = \boldsymbol{k}^3\chi(\boldsymbol{k})_{\mathrm{N/O}} + \boldsymbol{k}^3\chi(\boldsymbol{k})_{\mathrm{C}} + \boldsymbol{k}^3\chi(\boldsymbol{k})_{\mathrm{Ru}}$. The total $\boldsymbol{k}^3\chi(\boldsymbol{k})_{\mathrm{calcd}}$ oscillation was compared with the filtered $\boldsymbol{k}^3\chi(\boldsymbol{k})_{\mathrm{obsd}}$ oscillation to confirm the reliability of the present analyses (Figure 5b). The structural parameters derived from EXAFS analyses are summarized in Table 5. The Ru−Ru distances of **1**−**4** determined by EXAFS analyses by using theoretical parameters for $F_i(\boldsymbol{k})$ and $\Phi_i(\boldsymbol{k})$ fall within the range of 3.42−3.44 Å. The dinuclear core is hardly affected by the carboxylato ligands. The Ru···Ru distances of **1**−**3** from

Table 4. Selected Bond Distances (Å) and Angles (deg) for Na[Ru$_2$(dhpta)(μ-O$_2$CCH$_3$)$_2$] (**4**)[a]

Bond Distances			
Ru(1)···Ru(2)	3.433(3)		
Ru(1)−O(1)	1.98(2)	Ru(1)−O(3)	2.05(2)
Ru(1)−O(9)	1.93(1)	Ru(1)−O(11)	2.10(2)
Ru(1)−O(21)	2.07(2)	Ru(1)−N(1)	1.96(2)
Ru(2)−O(5)	1.97(2)	Ru(2)−O(7)	2.06(2)
Ru(2)−O(9)	1.95(2)	Ru(2)−O(12)	2.12(2)
Ru(2)−O(22)	2.04(2)	Ru(2)−N(2)	2.00(2)
Bond Angles			
O(1)−Ru(1)−O(3)	89.8(7)	O(1)−Ru(1)−O(9)	99.0(6)
O(1)−Ru(1)−O(11)	90.0(6)	O(1)−Ru(1)−O(21)	174.7(7)
O(1)−Ru(1)−N(1)	86.1(8)	O(3)−Ru(1)−O(9)	165.6(7)
O(3)−Ru(1)−O(11)	93.0(7)	O(3)−Ru(1)−O(21)	85.0(7)
O(3)−Ru(1)−N(1)	83.7(7)	O(9)−Ru(1)−O(11)	98.4(6)
O(9)−Ru(1)−O(21)	86.3(7)	O(9)−Ru(1)−N(1)	85.5(8)
O(11)−Ru(1)−O(21)	89.4(7)	O(11)−Ru(1)−N(1)	174.9(8)
O(21)−Ru(1)−N(1)	94.1(8)	O(5)−Ru(2)−O(7)	89.9(6)
O(5)−Ru(2)−O(9)	98.4(6)	O(5)−Ru(2)−O(12)	89.8(6)
O(5)−Ru(2)−O(22)	175.2(7)	O(5)−Ru(2)−N(2)	84.6(7)
O(7)−Ru(2)−O(9)	166.0(7)	O(7)−Ru(2)−O(12)	93.1(6)
O(7)−Ru(2)−O(22)	85.3(7)	O(7)−Ru(2)−N(2)	84.0(7)
O(9)−Ru(2)−O(12)	98.1(6)	O(9)−Ru(2)−O(22)	86.3(7)
O(9)−Ru(2)−N(2)	85.6(7)	O(12)−Ru(2)−O(22)	90.5(7)
O(12)−Ru(2)−N(2)	173.8(8)	O(22)−Ru(2)−N(2)	94.8(8)
Ru(1)−O(11)−C(31)	133(2)	Ru(2)−O(12)−C(31)	129(2)
Ru(1)−O(21)−C(21)	132(2)	Ru(2)−O(22)−C(21)	141(2)

[a] Estimated standard deviations are given in parentheses. See Figure 4 for atom labels.

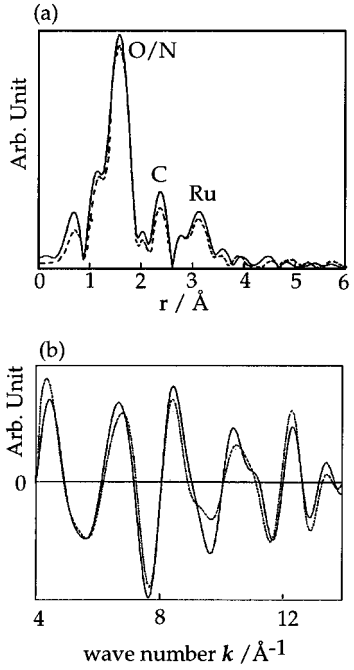

Figure 5. (a) Fourier transforms over $\boldsymbol{k} = 4-14$ Å^{-1} of the $\boldsymbol{k}^3$-weighted EXAFS data (before phase shift correction) for **4** in powdered form (—) and in H$_2$O (- -). (b) Curve fit over the range of $\boldsymbol{k} = 4-14$ Å^{-1} to the Fourier filtered data for **1** (powder); filtered EXFAS data (—) and calculated data (- -).

Table 5. Structural Parameters Derived from EXAFS Analysis for $Na[Ru_2(dhpta)(\mu\text{-}O_2CR)_2]$ (**1**−**4**)

	theoretical analysis				empirical analysis	
complex state	shell	r, Å[a]	N[b]	s	r, Å[c]	N[b]
1 powder (R = C_6H_5)	Ru-O/N	2.03	5.6	0.043		
	Ru-C	2.84	5.6	0.028		
	Ru−Ru	3.44	1.0	0.059	3.44	0.9
1 in H_2O	Ru-O/N	2.03	5.3	0.041		
	Ru-C	2.88	4.5	0.034		
	Ru−Ru	3.43	0.9	0.057	3.42	0.9
2 powder (R = *p*-OHC_6H_4)	Ru-O/N	2.04	6.1	0.048		
	Ru-C	2.83	5.5	0.032		
	Ru−Ru	3.44	1.0	0.062	3.43	0.9
2 in H_2O	Ru-O/N	2.04	5.7	0.042		
	Ru-C	2.82	4.7	0.040		
	Ru−Ru	3.44	1.1	0.067	3.42	0.8
3 powder (R = *p*-$NH_2C_6H_4$)	Ru-O/N	2.03	5.9	0.042		
	Ru-C	2.84	6.1	0.035		
	Ru−Ru	3.45	1.0	0.065	3.43	0.8
4 powder (R = CH_3)	Ru-O/N	2.04	6.0[d]	0.051		
	Ru-C	2.84	6.0[d]	0.030		
	Ru−Ru	3.44	1.0[d]	0.057	(3.433)[e]	(1.0)[e]
4 in H_2O	Ru-O/N	2.04	5.9	0.048		
	Ru-C	2.83	4.9	0.028		
	Ru−Ru	3.42	1.0	0.056	3.42	1.0

[a] Estimated errors are ±0.03 Å for the first shell (Ru−O/N) and ±0.04 Å for the second (Ru−C) and third (Ru−Ru) shells. [b] Estimated errors are ±0.3. [c] Estimated errors are ±0.01 Å. [d] Referenced to complex **4** (powder). [e] Values are determined by X-ray crystallography and are used as a model compound.

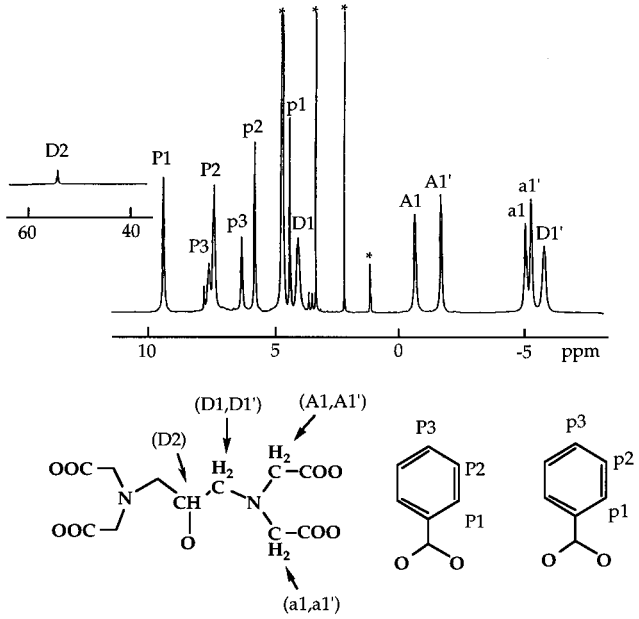

Figure 6. ^1H NMR spectrum of $Na[Ru_2(dhpta)(\mu\text{-}O_2CC_6H_5)_2]$ (**1**) in D_2O and peak assignments. Peaks with asterisks are corresponding to solvents and inpurities.

the analyses with empirical parameters for $F_i(\boldsymbol{k})$ and $\Phi_i(\boldsymbol{k})$, which were derived from that of **4**, are also in good accord with those with theoretical ones.

NMR Spectroscopic Analyses. The ^1H NMR spectra of **1**−**4** in D_2O showed isotropically shifted features in the range of −5 to +54 ppm, owing to the paramagnetism of Ru(III) ions. Resonances for the methine proton of dhpta were shifted to δ 54.26 (**1**), 52.97 (**2**), 50.88 (**3**), and 50.81 (**4**). In particular, the resonances observed in the ^1H NMR spectrum of **1** were completely assigned as shown in Figure 6 and Table 6 by means of $^1H-^1H$, $^{13}C-^1H$ COSY and noise- and nondecoupled ^{13}C NMR techniques. A broad resonance for the methine proton of dhpta was observed at δ 54.26, as mentioned above, and those for the methylene protons of the propane unit, at δ −5.82 and 4.04. Two sets of methylene peaks for the acetate arms of dhpta appeared at δ −0.63, −1.69 (A1) and −5.06, −5.30 (a1).

Table 6. ^1H and ^{13}C NMR NMR Spectral Data for $Na[Ru_2(dhpta)(\mu\text{-}O_2CC_6H_5)_2]$ (**1**)

assignment[a]	^1H NMR δ/ppm (*J*/Hz)[b]	^{13}C NMR δ/ppm[b,c]
P1	9.41	135.9
P2	7.43	132.7
P3	7.63	135.6
P4		117.2
p1	4.39	126.4
p2	5.82	129.1
p3	6.33	133.1
p4		112.5
D1, D1′	4.04, −5.82	86.9
D2	54.26	63.6
A1, A1′	−0.63, −1.69 (16.8)[d]	53.3
a1, a1′	−5.06, −5.30	58.4
P0, p0, A0, a0		142.3, 166.4, 174.0[e]

[a] See Figures 6 and 7 for the notations of H and C atoms. [b] Measured in D_2O at room temperature. Chemical shifts are calibrated to TMS as an external reference. [c] Measured with noise-decoupled mode. [d] Doublet. [e] Not unambiguously assigned.

Two environmentally different benzoate groups were also confirmed in the range of δ 4.39−9.41 as denoted with P1−3 and p1−3. The assignments of the ^{13}C NMR spectrum of **1** were also unambiguously established except for the carbonyl carbons of dhpta and benzoate ligands (Figure 7 and Table 6). These NMR spectral features were in agreement with the crystal structures, involving two environments for the acetate parts of dhpta and the carboxylate ligands in C_s symmetry.

Magnetic Properties. Complexes **1**−**4** are paramagnetic at room temperature with magnetic moments of 0.87−1.1 μ_B/Ru(III) ion which are smaller than is expected for a low-spin electronic structure owing to the intramolecular antiferromagnetic interaction described below. The temperature-dependent molar susceptibiliy of the (μ-alkoxo)bis(μ-carboxylate)diruthenium complexes **1**−**4** in the range 78−320 K showed an antiferromagnetic intramolecular spin coupling which was analyzed by the general isotropic exchange Hamiltonian, $H = -2JS_1 \cdot S_2$ ($S_1 = S_2 = {}^1/_2$), to afford $-J = 310-470$ cm^{-1}, $g = 2.0-2.4$, and TIP = $118-274 \times 10^{-6}$ (Figure 8 and Table 7). The obtained *g* values are highly anisotropic and still fall within the range reported for diruthenium(III) complexes.[2b] The anti-

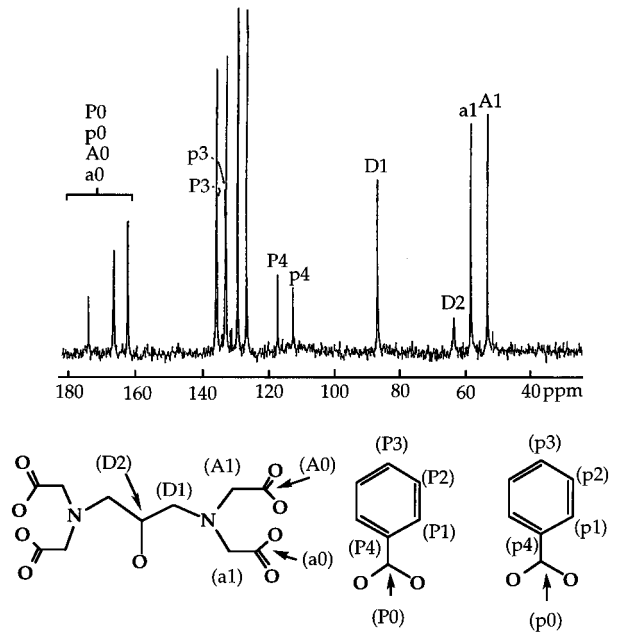

Figure 7. ^{13}C NMR spectrum of Na[Ru$_2$(dhpta)(μ-O$_2$CC$_6$H$_5$)$_2$] (**1**) in D$_2$O and peak assignments.

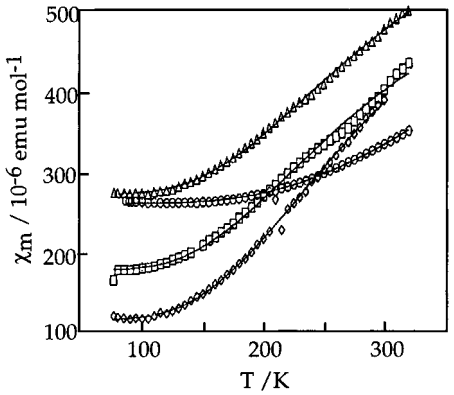

Figure 8. Temperature dependence of the magnetic susceptibility data of Na[Ru$_2$(dhpta)(μ-O$_2$CR)$_2$]: **1** (□); **2** (◇); **3** (△); **4** (○). The solid lines are calculated with eq 1 in the text.

Table 7. Magnetic Parameters Derived from the Fit to Temperature-dependent Molar Susceptibility of Na[Ru$_2$(dhpta)(μ-O$_2$CR)$_2$] (**1**−**4**) and Related Complexes

complex	R	g	$-J$, cm^{-1}	$10^6 \times$ TIP, emu/mol
1	C_6H_5	2.0	310	180
2	p-OHC_6H_4	2.2	312	118
3	p-$NH_2C_6H_4$	2.0	330	274
4	CH_3	2.4	470	263
[Ru$_2$(Me$_3$tacn)$_2$(μ-O)(O$_2$CCH$_3$)$_2$]$^{2+}$, **5**[a]		diamagnetic		
[Ru$_2$(Me$_3$tacn)$_2$(μ-OH)(O$_2$CCH$_3$)$_2$]$^{3+}$, **6**[a]		2.4	218	0

[a] Reference 2a,b.

ferromagnetic coupling constants ($-J$) are lager than that of [Ru$_2$(μ-OH)(μ-O$_2$CCH$_3$)$_2$(Me$_3$tacn)$_2$](PF$_6$)$_3$ ($-J$ = 218 cm^{-1}).[2a,b] These antiferromagnetic interactions observed in the {Ru$^{III}_2$(μ-alkoxo)(μ-carboxylate)$_2$} and {Ru$^{III}_2$(μ-hydroxo)(μ-carboxylate)$_2$} complexes are interestingly compared with diamagnetic properties of {Ru$^{III}_2$(μ-oxo)(μ-carboxylate)$_2$} complexes,[2a,b] suggesting that the spin−spin coupling interaction between two Ru(III) ions is dramatically affected by the monoatom-bridging ligand. Previously, we reported the magnetic properties of (dhpta)iron(III) dimers with a bridgeing carboxylate, [Fe$_2$(dhpta)(μ-O$_2$CR)(H$_2$O)$_2$] (R = p-OHC_6H_4, $CH_2CH{=}CH_2$, p-$NH_2C_6H_4$, CH_2CH_2Br, $CH{=}CHCH_3$).[20] Weak antiferromagnetic interactions were found independent of the bridging carboxylate ligands. In the present diruthenium system, however, the acetate complex **4** showed stronger antiferromagnetic coupling in comparison with benzoate analogues **1**−**3**.

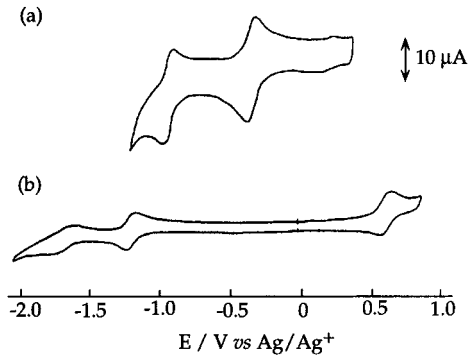

Figure 9. Cyclic voltammograms for Na[Ru$_2$(dhpta)(μ-O$_2$CC$_6$H$_5$)$_2$] (**1**): (a) 1 mM H$_2$O solution (pH = 6.88) at a scan rate of 50 mV s^{-1}; (b) 0.5 mM DMF solution at a scan rate of 100 mV s^{-1}. Redox potential data are shown in Table 9.

Electrochemical Study. The electrochemistry of **1**−**4** in water and DMF was studied by cyclic voltammetry (Table 8). In all cases in water, two reduction processes were observed at ca. −0.34 V ($E^1_{1/2}$) and ca. −0.94 V ($E^2_{1/2}$) *vs* Ag/AgCl (Figure 9a). No oxidation wave was observed within the solvent limits. The reduction potentials, $E^1_{1/2}$ and $E^2_{1/2}$, were independent on the carboxylate ligands. The former couple was reversible with $i^1_{pa}/i^1_{pc} \sim 1$ for scan rates (v) between 50 and 500 mVs^{-1} and the ratio $i^1_p/v^{1/2}$ was constant in accord with a diffusion-controlled process. The potential separations, $\Delta E^1 = |E^1_{pa} - E^1_{pc}|$, were in the range 62−89 mV indicating an one-electron transfer per dimer. The latter wave was quasi-reversible with $i^2_{pa} < i^2_{pc}$ preventing further detailed discussion, however, i^2_{pc} was nearly equal to i^1_{pc}. The observed redox couples were presumably corresponding to the two stepwise one-electron reduction processes designated in eq 3.

$$[Ru^{III}_2(dhpta)L_2]^- \overset{E^1_{1/2}\ +e^-}{\underset{-e^-}{\rightleftharpoons}} [Ru^{II}Ru^{III}(dhpta)L_2]^{2-} \overset{E^2_{1/2}\ +e^-}{\underset{-e^-}{\rightleftharpoons}} [Ru^{II}_2(dhpta)L_2]^{3-} \quad (3)$$

$$L = RCO_2^-$$

The most remarkable feature is the large separation between the two redox potentials $E^1_{1/2}$ and $E^2_{1/2}$ ($\Delta E_{1,2} = |E^1_{1/2} - E^2_{1/2}| = 0.60$ V). The conproportionation constant K_c for eq 4, which was known to be calculated with eq 5, is 2×10^{10}. The K_c

$$[Ru^{III}_2(dhpta)L_2]^- + [Ru^{III}_2(dhpta)L_2]^{3-} \overset{K_c}{\rightleftharpoons} 2[Ru^{II}Ru^{III}(dhpta)L_2]^{2-} \quad (4)$$

$$L = RCO_2^-$$

$$K_c = \exp\left(\frac{\Delta E_{1,2} n_1 n_2 F}{RT}\right) \quad (5)$$

values obtained were larger than that of [Ru$_2$(tacn)$_2$(μ-OH)$_2$(OC$_2$-CH$_3$)]$^{3+}$ (2×10^8) (**11**).[18,21] From these, the mixed-valence diruthenium species [Ru^{II}Ru^{III}(dhpta)(μ-O$_2$CR)$_2$]$^{2-}$ (**12**) is ex-

(20) Kato, M.; Yamada, Y.; Inagaki, T.; Mori, W.; Sakai, K.; Tsubomura, T.; Sato, M.; Yano, S. *Inorg. Chem.* **1995**, *34*, 2645.
(21) Neubold, R.; Vedova, B. S. P. C. D.; Wieghardt, K.; Nuber, B.; Weiss, J. *Inorg. Chem.* **1990**, *29*, 3355.

Table 8. Electrochemical Data for $Na[Ru_2(dhpta)(\mu\text{-}O_2CR)_2]$ (**1**−**4**)

complex	R	solv[a,b]	$E^2_{1/2}$, V[c]	$E^1_{1/2}(\Delta E)$, V[d]	E_{ox}, V[c]	$\Delta E_{1,2}$, V[e]	K_c[f]
1	C_6H_5	H_2O[a]	−0.92	−0.32 (62)		0.60	2.0×10^{10}
		DMF[b]	−1.64	−1.24 (80)	0.59	0.40	5.8×10^{6}
2	p−OHC_6H_4	H_2O[a]	−0.94	−0.34 (67)		0.60	2.0×10^{10}
		DMF[b]	−1.70	−1.20 (70)	0.60	0.50	2.8×10^{8}
3	p−$NH_2C_6H_4$	H_2O[a]	−0.95	−0.35 (70)		0.60	2.0×10^{10}
		DMF[b]	−1.72	−1.20 (70)	0.60	0.52	6.2×10^{8}
4	CH_3	H_2O[a]	−0.93	−0.33 (89)		0.60	2.0×10^{10}
		DMF[b]	−1.81	−1.28 (99)	0.57	0.53	9.1×10^{8}

[a] Cyclic voltammograms were measured in phosphate buffer (pH 6.88) containing 0.1 M Na_2SO_4 by using a glassy carbon electrode at 20 °C with a scanning rate of 50 mVs^{-1}. Potentials were referenced to Ag/AgCl. [b] Cyclic voltammograms were measured in DMF containing 0.1 M [n-Bu_4N][PF_6] at room temperature by using a glassy carbon electrode with a scanning rate of 100 mVs^{-1}. Potentials were referenced to Ag/$AgPF_6$. [c] Irreversible. [d] Reversible. ΔE is potential separation, $|E^1_{pa} - E^1_{pc}|$, in mV. [e] $\Delta E_{1,2} = |E^1_{1/2} - E^2_{1/2}|$. [f] The conproportionation constant for eq 4 calculated with $K_c = \exp[\Delta E_{1,2} n_1 n_2 F/RT]$ as defined in eq 5.

pected to be more stable than the corresponding dimer from **11**, and the unpaired electron in **12** should be considerably delocalized. The cyclic voltammograms of **1**−**4** in DMF also exhibited two reduction processes ascribable to the two stepwise one-electron transfers shown in eq 3 as well as an oxidation process tentatively corresponding to the one-electron oxidation of $[Ru^{III}_2(dhpta)(O_2CR)_2]^- \leftrightarrow [Ru^{III}Ru^{IV}(dhpta)(O_2CR)_2]$ (Figure 9b and Table 8). The $\Delta E_{1,2}$ values of 0.40−0.53 V afforded K_c ranging from 5.8×10^6 to 9.1×10^8, implying that the mixed valence $Ru^{II}Ru^{III}$ species are still stable in DMF. It should be noted that the second potentials $E^2_{1/2}$ in DMF reflected the electron-donating ability of the carboxylate substituent groups, the $E^2_{1/2}$ values showing an approximate correlation to the pK_a values of RCO_2H.

A potentiostatic electrolysis of **2** in phosphate buffer (pH 6.88) at −0.7 V *vs* Ag/AgCl consumed about 1 F per mol of dimer, and the color of the solution changed from reddish violet to green. While the broad characteristic band centered at ∼800 nm in the electronic absorption spectrum of the solution was tentatively corresponding to an intervalence charge-transfer transition of the mixed-valence species **12**, as compared with those of $[Ru^{II}Ru^{III}(\mu\text{-}OH_2)Cl(MeCN)(\mu\text{-}O_2CR)_2(O_2CR)_2(PPh_3)_2]$ (R = p-$OMeC_6H_4$, λ_{max} 960 nm; R = C_6H_5, λ_{max} 880 nm),[5f,g] a detailed spectroscopic analysis could not be performed due to absorptions by solvent water in the near-infrared region. The similar electrolyses were carried out in DMF at −1.5 V for **1**, **3**, and **4**, and at −1.4 V for **2** *vs* Ag/$AgPF_6$ to generate the $Ru^{II}Ru^{III}$ mixed-valence species **12**. The color of the solution turned to orange−dark green monitored by electronic absorption spectroscopy (0.5−30 kcm^{-1}). The one-electron reduced complexes, $[Ru^{II}Ru^{III}(dhpta)(\mu\text{-}O_2CR)_2]^{2-}$ (**12**), were immediately oxidized by air to regenerate $[Ru^{III}_2(dhpta)(\mu\text{-}O_2CR)_2]^-$ (**1**−**4**). Although complexes **12** were not isolated despite an attempt to do so, the molar concentrations of **12** could be determined on the basis of the Ru^{III}_2 starting complexes restored The electronic absorption spectrum of $[Ru^{II}Ru^{III}(dhpta)(\mu\text{-}O_2CR)_2]^{2-}$ (**12**, R = CH_3) together with that of **4** are illustrated in Figure 10a. Two broad bands centered around 5.69 (band I) and 11.9 kcm^{-1} (band II) were assignable to intervalence charge transfer bands because they are absent in the electronic spectrum of $[Ru^{III}_2(dhpta)(\mu\text{-}O_2CCH_3)_2]^-$ (**4**). The other mixed-valence complexes from **1**−**3** also exhibited the similar spectroscopic aspects (Table 9). The lower-energy IT band (band I) was analyzed by Gaussian curve fitting to determined the energy of the band maximum ν_{max}, the maximum extinction coefficient ϵ_{max}, and the half-height width $\Delta\nu_{1/2}$ (Figure 10b and Table 9). The electron exchange integral H_{ad}, which is a good index to represent the magnitude of interaction between the metal centers, were calculated according to Hush's theory (eq 6)[22,23] as 640−

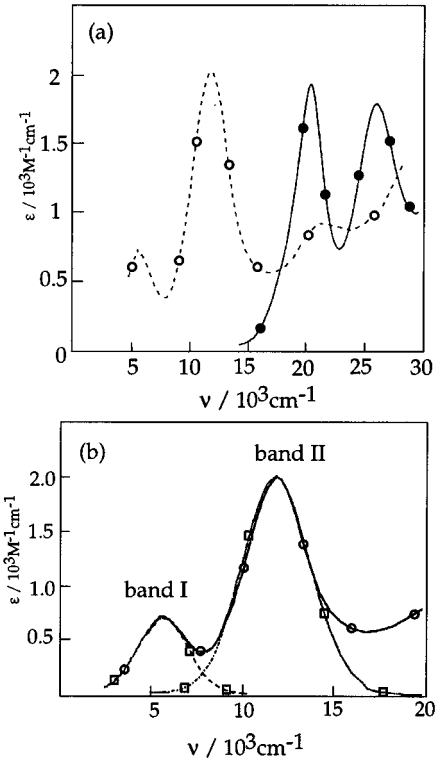

Figure 10. (a) Electronic absorption spectra of $[Ru_2(dhpta)(\mu\text{-}O_2CCH_3)]^{n-}$ (n = 1, 2) in DMF, the mixed-valence species, $[Ru_2(dhpta)(O_2CCH_3)_2]^{2-}$, generated by the potentiostatic electrolysis of **4** (○), and $Na[Ru_2(dhpta)(\mu\text{-}O_2CCH_3)_2]$ (**4**) (●). (b) Fitting of the intervalence charge transfer bands (band I and band II) of $[Ru_2(dhpta)(O_2CCH_3)_2]^{2-}$: observed spectrum (○); fitted data to band I (□); fitted data to band II (□).

870 cm^{-1}. The Ru−Ru interatomic distances (r) used in the

$$H_{ad} = 2.05 \times 10^{-2} \sqrt{\frac{\epsilon_{max} \Delta\nu_{1/2}}{\nu_{max}}} \left(\frac{\nu_{max}}{r}\right) \qquad (6)$$

calculation were derived from EXAFS analyses. The values of H_{ad} indicate weak metal−metal interactions and are comparable to those of $[(NH_3)_5Ru(\mu\text{-}3,3'\text{-bpy})Ru(NH_3)_5]^{5+}$ (400 cm^{-1})[23,25] and $[Ru_2(OH_2)Cl(MeCN)(O_2CC_6H_4\text{-}p\text{-}OMe)_4(PPh_3)]$ (965 cm^{-1})[5f,g] which were reported as Class II type mixed-valence diruthenium complexes.[26] As to the higher-energy IT band (band II), we did not analyze it in detail in this report

(22) Creutz, C. *Prog. Inorg. Chem.* **1983**, *30*, 1.
(23) Hush, N. S. *Prog. Inorg. Chem.* **1967**, *8*, 391.
(24) Rieder, K.; Taube, H. *J. Am. Chem. Soc.* **1977**, *99*, 7891.
(25) Tanner, M.; Ludi, A. *Inorg. Chem.* **1981**, *20*, 2348.
(26) Robin, M. B.; Day, P. *Adv. Chem. Radiochem.* **1967**, *10*, 247.

Table 9. Spectral Data of Intervalence Charge Transfer Bands of $[Ru_2(dhpta)(\mu\text{-}O_2CR)_2]^{2-}$ (**12**)

	R = CH_3	R = C_6H_5	R = *p*-OHC_6H_4	R = *p*-$NH_2C_6H_4$
		Band I		
$\nu_{max,obsd}$[a]	5.7	5.5	5.6	5.7
$\nu_{max,calcd}$[a]	4.4	5.6	4.8	4.1
ϵ_{max}[b]	0.69	1.10	0.89	0.64
$\Delta\nu_{1/2,obsd}$[a]	3.2	3.6	3.3	3.1
$\Delta\nu_{1/2,calcd}$[a]	3.6	3.6	3.6	3.6
H_{ad}[c]	0.67	0.87	0.82	0.63
		Band II		
$\nu_{max,obsd}$[a]	11.9	11.6	11.7	11.8
ϵ_{max}[b]	2.03	2.72	2.79	2.70

[a] In 10^{-3} cm^{-1}. [b] In 10^{-3} M^{-1} cm^{-1}. [c] In cm^{-1}.

because its alternative assignment to a LMCT band was not thoroughly ruled out.

In conclusion, the dinuclear ruthenium(III) complexes (**1**−**4**) involving {Ru_2(μ-alkoxo)(μ-carboxylato)$_2$} core were successfully prepared by using a dinucleating ligand, 1,3-diamino-2-hydroxypropanetetraacetic acid ($dhptaH_5$), and were characterized by X-ray crystallography and EXAFS analysis. Complexes **1**−**4** are soluble and retain the dinuclear structure in water and DMF, and thus provide a good platform to elucidate redox properties of the diruthenium center. Two stepwise one-electron reductions, $Ru^{III}Ru^{III} \leftrightarrow Ru^{III}Ru^{II} \leftrightarrow Ru^{II}Ru^{II}$ were observed in cyclic voltammograms of **1**−**4**, and the large separation between the two redox potentials indicated that the mixed-valence diruthenium(III,II) complexes of dhpta are fairly stable. Mixed-valence diruthenium complexes, [Ru_2(dhpta)-(μ-$O_2CR)_2]^{2-}$, were generated by electrochemical reduction of **1**−**4**, and the spectroscopic analysis demonstrated a weak metal−metal interaction as were observed in Class II type complexes.

Acknowledgment. We thank Profs. Motowo Yamaguchi, Takamichi Yamagishi, and Tetsuo Nagano for their helpful discussion. This work was partially supported by a Grant-in-Aid for Scientific Research from the Ministry of Education of Japan and Grants from Nippon Itagarasu Foundation.

Supporting Information Available: Tables of crystallographic data, atomic positional and thermal parameters, and bond distances and angles for **4** and **4′**·1.5H_2O and figures showing the raw EXAFS data and Fourier transforms of all samples **1**−**4** (15 pages). Ordering information is given on any current masthead page.

IC960435G